XVII IMEKO WORLD CONGRESS
Metrology for a Sustainable Development
September, 17–22, 2006 Rio de Janeiro, Brazil

CALIBRATION OF A MEMS INERTIAL MEASUREMENT UNIT

Isaac Skog[1], *Peter Händel*[2]

[1] Signal Processing Lab, Royal Institute of Technology, Stockholm, Sweden, skog@s3.kth.se
[2] Signal Processing Lab, Royal Institute of Technology, Stockholm, Sweden, ph@s3.kth.se

Abstract: An approach for calibrating a low-cost IMU is studied, requiring no mechanical platform for the accelerometer calibration and only a simple rotating table for the gyro calibration. The proposed calibration methods utilize the fact that ideally the norm of the measured output of the accelerometer and gyro cluster are equal to the magnitude of applied force and rotational velocity, respectively. This fact, together with model of the sensors is used to construct a cost function, which is minimized with respect to the unknown model parameters using Newton's method. The performance of the calibration algorithm is compared with the Cramér-Rao bound for the case when a mechanical platform is used to rotate the IMU into different precisely controlled orientations. Simulation results shows that the mean square error of the estimated sensor model parameters reaches the Cramér-Rao bound within 8 dB, and thus the proposed method may be acceptable for a wide range of low-cost applications.

Keyword: Inertial measurement unit, MEMS sensors, Calibration.

1. INTRODUCTION

The development in micro-electro-mechanical system (MEMS) technology has made it possible to fabricate cheap single chip accelerometer and gyro sensors, which have been adopted into many applications where traditionally inertial sensors have been too costly. For example the MEMS sensors have made it possible to construct low cost global navigation satellite system (GNSS) aided inertial navigation systems (INS) for monitoring vehicle behavior [1]. The obtained accuracy and convergence time of a GNSS aided INS is highly dependent on the quality of the IMU sensors output [2], and therefore a calibration of the IMU is critical for the over all system performance.

Traditionally the calibration of an IMU has been done using a mechanical platform, turning the IMU into different precisely controlled orientations and at known rotational velocities [3, 4, 5]. At each orientation and during the rotations the output of the accelerometers and gyros are observed and compared with the precalculated gravity force and rotational velocity, respectively. However, the cost of a mechanical platform can many times exceed the cost of developing and constructing a MEMS sensor based inertial measurement unit. Therefore, in [6] a calibration procedure using a optical tracking system is studied. In [4, 7] calibration procedures for the accelerometer cluster, where the requirements of a precise control of the IMU's orientation is relaxed are proposed.

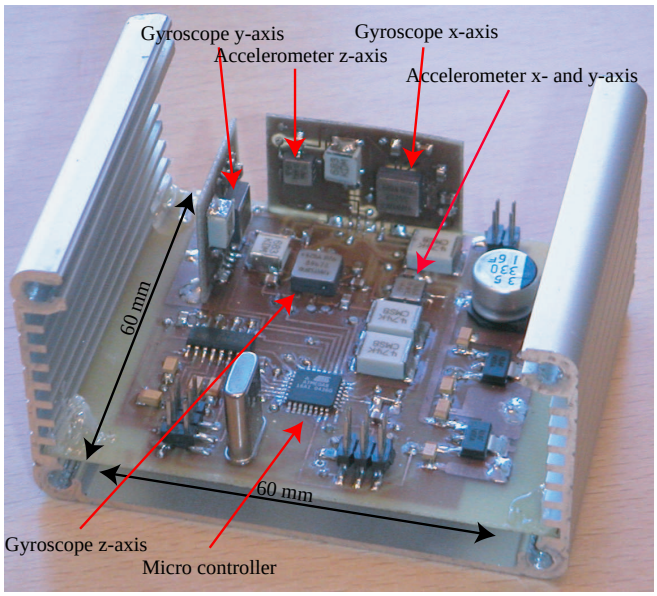

Fig. 1: The in-house constructed inertial measurement unit. In the upper part of the picture the three gyros and the double axed and single axed accelerometer can be seen. In the lower part of the picture the micro-controller can be seen, responsible for sampling of the sensors. Altogether the IMU measures 60×60×25 mm.

These calibration methods utilize the fact that ideally the norm of the measured output of the accelerometer and gyro cluster should be equal to the magnitude of the applied force and rotational velocity, respectively. However there are one major disadvantage with such a method; not all sensor parameters of the IMU are observable. This implies that these parameters (errors sources) most be taken into account in the integration of the IMU and GNSS data, increasing the computational complexity of the data fusion algorithm.

In this paper the problem of calibrating a low cost IMU when the precise orientation of the IMU is unknown is studied. In Section 2, a sensor model applicable both to the accelerometer and gyro sensor cluster are described and related to the in-house constructed IMU. Next, in Section 3 the estimation of the model parameters when the precise orientation of the IMU is unknown is studied and a cost function is proposed. The cost function is numerically minimized using Newton's method. In Section 4, the Cramér Rao lower bound (CRLB) for the parameter estimation problem is derived when the orientation of the platform is precisely con-

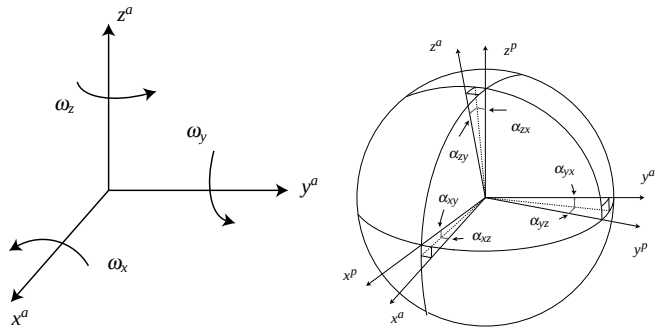

(a) Accelerometer and gyro sensitivity axes. **(b) Accelerometer and platform coordinate axes.**

Fig. 2: The accelerometer sensitivity axes $\{x^a, y^a, z^a\}$ are mounted to span a 3-dim space and the gyros to measure the angular velocities $\{\omega_x, \omega_y, \omega_z\}$ around these axes. The nonorthogonal axes of accelerometer cluster can be aligned with the orthogonal platform axes $\{x^p, y^p, z^p\}$ through the six angles $\{\alpha_{xy}, \alpha_{xz}, \alpha_{yx}, \alpha_{yz}, \alpha_{zx}, \alpha_{zy}\}$.

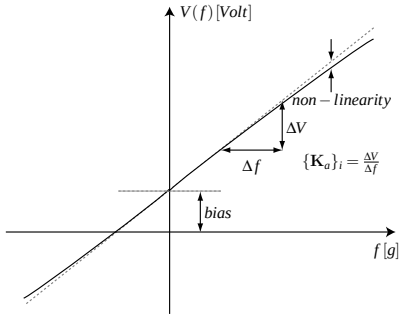

Fig. 3: The relationship between the output voltage of the accelerometer(gyro) and the measured force(angular rate) is modelled as a linear function, describing the scaling and bias of the sensors.

trolled, serving as a bound when evaluating the performance of the estimator. In Section 5, results from a Monte Carlo simulation of the proposed calibration approach is presented. Moreover, the in-house IMU is calibrated, and the estimated model parameters are examined. The conclusions are drawn in Section 6.

2. SENSOR ERROR MODEL

An inertial measurement unit has been constructed around MEMS accelerometers and gyros from Analog-Devices, see Figure 1. The double and single axed accelerometers ADXL 203 and ADXL 103, respectively have been mounted so their sensitivity axes $\{x^a, y^a, z^a\}$ span a three dimensional space. The three ADXRS 150 gyros are mounted to measure the angular velocities $\{\omega_x, \omega_y, \omega_z\}$ around the accelerometers sensitivity axes, see Figure 2(a). This gives a six degree-of-freedom IMU capable of measuring accelerations and angular rates between $\pm 15[m/s^2]$ and $\pm 150[^\circ/s]$, respectively. Ideally, the sensor sensitivity axes should be orthogonal, but due to the impreciseness in the construction of the IMU this is seldom the case [6]. If the nonorthogonal sensitivity axes of the accelerometer clusters differ only by "small" angles from the orthogonal set of platform coordinate axes, see Figure 2(b), the specific force in accelerometer cluster coordinates can be transformed into specific force estimates in platform coordinates as [8]

$$\mathbf{s}^p = \mathbf{T}_a^p \mathbf{s}^a, \qquad \mathbf{T}_a^p = \begin{pmatrix} 1 & -\alpha_{yz} & \alpha_{zy} \\ \alpha_{xz} & 1 & -\alpha_{zx} \\ -\alpha_{xy} & \alpha_{yx} & 1 \end{pmatrix} \quad (1)$$

where $\mathbf{s}^p$ and $\mathbf{s}^a$ denote the specific force in platform and accelerometer coordinates, respectively. Here α_{ij} is the rotation of the i-th accelerometer sensitivity axis around the j-th platform axis. By defining the platform coordinate system so that the platform coordinate axis x^p coincides with the x^a accelerometer sensitivity axis, and so that the y^p axis is lying in the plane spanned by x^a and y^a the angles $\{\alpha_{xz}, \alpha_{xy}, \alpha_{yx}\}$ become zero. That is (1) is reduced to

$$\mathbf{s}^p = \mathbf{T}_a^p \mathbf{s}^a, \qquad \mathbf{T}_a^p = \begin{pmatrix} 1 & -\alpha_{yz} & \alpha_{zy} \\ 0 & 1 & -\alpha_{zx} \\ 0 & 0 & 1 \end{pmatrix}. \quad (2)$$

Because the platform coordinate axes already have been defined, six small rotations around the platforms axes are required to define the rotation from the gyro input axes to the platform axes. That is, three rotations are required to make the sensitivity axes of the gyro cluster orthogonal and three rotations are needed to align the orthogonal coordinate axes with the platform coordinate axes. The relationship reads

$$\omega_{ip}^p = \mathbf{T}_g^p \omega_{ig}^g, \qquad \mathbf{T}_g^p = \begin{pmatrix} 1 & -\gamma_{yz} & \gamma_{zy} \\ \gamma_{xz} & 1 & -\gamma_{zx} \\ -\gamma_{xy} & \gamma_{yx} & 1 \end{pmatrix}. \quad (3)$$

Here γ_{ij} is the small rotation of the i-th gyro sensitivity axis around the j-th platform axis. This may equivalently be written as

$$\omega_{ip}^p = \mathbf{R}_o^p \mathbf{T}_g^o \omega_{ig}^g, \qquad \mathbf{T}_g^o = \begin{pmatrix} 1 & -\gamma_{yz} & \gamma_{zy} \\ 0 & 1 & -\gamma_{zx} \\ 0 & 0 & 1 \end{pmatrix} \quad (4)$$

where $\mathbf{T}_g^o$ transforms the nonorthogonal gyro sensitivity axes into a set of orthogonal coordinate axes. The matrix $\mathbf{R}_o^p$ denotes the directional cosine matrix transforming the angular velocities in orthogonal sensitivity axes coordinates into platform coordinates.

The MEMS sensors output a voltage proportional to the physical quantities sensed by the sensors, acceleration and angular rates, respectively. The typical relationship between the output voltage and the physical quantity acting along the sensor sensitivity axes is given by the manufactures data sheet, but the true scaling varies between different specimens and with the input signal (due to inherent nonlinearities of the sensors). Moreover, there is often a small bias in the sensor output signal, that is even though there is no force acting onto the sensor, the sensors produces a non-zero output, see Figure 3. For the MEMS sensors used in our application the nonlinearities are in the order 0.1% of a best fit to a straight line and may therefore be neglected. Introduce the accelerometer scale factor matrix $\mathbf{K}_a$ and bias vector $\mathbf{b}_a$ defined as

$$\mathbf{K}_a = \mathrm{diag}(k_{x_a}, k_{y_a}, k_{z_a}), \qquad \mathbf{b}_a = [\, b_{x_a} \; b_{y_a} \; b_{z_a} \,]^T \quad (5)$$

where k_{i_a} and b_{i_a} are the unknown scaling and bias of the i-th accelerometer output, respectively. Further $(\cdot)^T$ denotes the transpose operation and $\mathrm{diag}(\cdot)$ the diagonal matrix with the elements given within the parentheses. The measured output of the accelerometer cluster may then be modelled as [4]

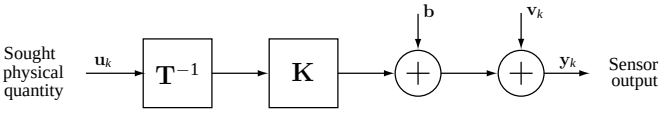

Fig. 4: Sensor model including misalignments $\mathbf{T}^{-1}$, scale factors $\mathbf{K}$, biases $\mathbf{b}$, and measurement noise $\mathbf{v}_k$.

$$\tilde{\mathbf{s}}^a = \mathbf{K}_a\,(\mathbf{T}_a^p)^{-1}\,\mathbf{s}^p + \mathbf{b}_a + \mathbf{v}_a \tag{6}$$

where $\mathbf{s}^a = (\mathbf{T}_a^p)^{-1}\mathbf{s}^p$ from (2) was employed. In (6), $\mathbf{v}_a$ is a noise term reflecting the measurement noise from the sensors. Applying the same model to the MEMS gyros, the output from the gyro-cluster may be written as

$$\begin{aligned}\tilde{\omega}_{ig}^g &= \mathbf{K}_g\,\omega_{ig}^g + \mathbf{b}_g + \mathbf{v}_g \\ &= \mathbf{K}_g\,(\mathbf{T}_g^o)^{-1}\,\mathbf{R}_p^o\,\omega_{ip}^p + \mathbf{b}_g + \mathbf{v}_g\end{aligned} \tag{7}$$

where $\mathbf{K}_g$ and $\mathbf{b}_g$ are the scale factor matrix and bias vector of the gyro-cluster, respectively. Further ω_{ip}^p is the true rotational rate of the IMU platform with respect to the inertial frame of reference and $\mathbf{v}_g$ is the gyro measurement noise. In the second equality in (7) the notation $\mathbf{R}_p^o = (\mathbf{R}_o^p)^{-1}$ has been used to denote the directional cosine matrix, rotating a vector from platform coordinates to the coordinate system associated with the orthogonal gyro sensitivity axes. Worth noting is that the misalignment matrices $\mathbf{T}_a^p$ and $\mathbf{T}_g^o$ are constant matrices only dependent on the physical mounting of the components. $\mathbf{K}_a, \mathbf{K}_g, \mathbf{b}_a$ and $\mathbf{b}_g$ may be split into a static part, a temperature varying and a random drift part [9]. The temperature varying and random drift part must be taken into account by the integration algorithm, fusing the GNSS and IMU data. Therefore the prime goal of the calibration is to estimate $\mathbf{T}_a^p$ and $\mathbf{T}_g^o$ and the static parts of the scale factors and biases.

Both the accelerometer and gyro cluster model fit into the more general signal model described by Figure 4. Here the input $\mathbf{u}_k$ corresponds to the specific force $\mathbf{s}^p$ at time k in the accelerometer cluster model or the angular velocity $\omega_{ip}^o = \mathbf{R}_p^o\,\omega_{ip}^p$ in the gyro cluster model.

3. CALIBRATION

Traditionally, a mechanical platform rotating the IMU into different precisely controlled orientations and angular rates has been used to calibrate IMU's. Then, observing the output $\mathbf{y}_k$ and the precalculated specific force or angular velocity $\mathbf{u}_k$ acting upon the IMU for 12 or more different orientations and rotation sequences, respectively it is straightforward to estimate the misalignment, scaling and bias [3, 4, 5]. Note, that there are 9 and 12 unknowns in the signal models, respectively - three scale factors, three biases, three orthogonal rotations and in addition for the gyro cluster the three rotations aligning the orthogonal gyro coordinate axes with the platform axes. The cost of a mechanical platform often exceeds the cost of developing and constructing a MEMS sensor based IMU. Therefore a calibration procedure is desirable where the requirements of a precisely controlled orientation of the IMU can be relaxed.

Based upon the signal model in Figure 4 the natural estimator for the sought input $\mathbf{u}_k$ based on the sensor output $\mathbf{y}_k$ is

$$\hat{\mathbf{u}}_k = \mathbf{h}(\mathbf{y}_k, \theta) = \mathbf{T}\,\mathbf{K}^{-1}(\mathbf{y}_k - \mathbf{b}) \tag{8}$$

where the sought parameters are collected in the parameter vector

$$\theta = \begin{bmatrix} k_x & k_y & k_z & \alpha_{yz} & \alpha_{zy} & \alpha_{zx} & b_x & b_y & b_z & \sigma^2 \end{bmatrix}^T. \tag{9}$$

In order to have a more unified notation throughout the paper the noise variance has been included in the parameter vector in (9). However, the proposed estimator does not depend on the noise variance and it can therefore be omitted in equations (8)-(15).

Ideally, independent of the orientation of the IMU, the magnitude of the measured gravity force and angular velocity should be equal to the magnitude of the apparent gravity force and applied angular velocity, respectively. Therefore, the squared error between the squared magnitude of the input $\mathbf{u}_k$ and the squared magnitude of the output from the compensated IMU output may serve as a cost function when calibrating the IMU. That is

$$\hat{\theta} = \underset{\theta}{\operatorname{argmin}}\{L(\theta)\} \tag{10}$$

where

$$L(\theta) = \sum_{k=0}^{K-1} (\|\mathbf{u}_k\|^2 - \|\mathbf{h}(\mathbf{y}_k, \theta)\|^2)^2. \tag{11}$$

Here, $K = MN$, where M is the number of orientations or rotations that the platform is exposed too and N the number of samples taken during each rotation or at each orientation. Still, since there are nine unknowns the platform must be exposed to nine or more orientations and rotations, respectively. However, the demand of a precise control of the orientation is relaxed. Worth noting when calibrating the gyros is that

$$\|\mathbf{u}_k\|^2 = \|\omega_{ip}^o\|^2 = \|\mathbf{R}_p^o\,\omega_{ip}^p\|^2 = \|\omega_{ip}^p\|^2 \tag{12}$$

where in the last equality the fact that the directional cosine matrix $\mathbf{R}_p^o$ is an orthonormal matrix, ie $(\mathbf{R}_p^o)^T(\mathbf{R}_p^o) = \mathbf{I}$, has been used. Therefore the three Euler angles relating the orthogonal coordinate axes of the gyro cluster and the platform coordinates are unobservable when the magnitudes are used to calibrate the IMU.

At each orientation of the IMU, the specific force acting along the accelerometers sensitivity axes are constant, i.e. the input $\mathbf{u}_k$ is constant during the N samples. This also holds for the gyro cluster model, if assuming that during each rotation of the IMU the rotation velocity is kept constant. The cost function may then be simplified as

$$L(\theta) = \sum_{m=0}^{M-1} (\|\overline{\mathbf{u}}^m\|^2 - \|\mathbf{h}(\overline{\mathbf{y}}^m, \theta)\|^2)^2 \tag{13}$$

where $\overline{\mathbf{u}}^m$ and $\overline{\mathbf{y}}^m$ are the input and sample mean at the m-th orientation and rotation, respectively. This reduced cost function may be minimized off-line using for example Newton's method, that is [10]

$$\hat{\theta}_{k+1} = \hat{\theta}_k + \left[\frac{\mathrm{d}^2 L(\theta)}{\mathrm{d}\theta\,\mathrm{d}\theta^T}\right]^{-1} \frac{\mathrm{d}L(\theta)}{\mathrm{d}\theta}\bigg|_{\theta=\hat{\theta}_k} \qquad (14)$$
$$\hat{\theta}_0 \in \text{domain of attraction.}$$

The cost function in (11) has several local optima and to ensure that the recursion (14) converges to the true parameters the search for the minima must be initialized with a θ in the domain of attraction of the global minima. According to the data sheet of the accelerometers the scale factors differ less then 6% from there nominal values (unit gain) and the biases are smaller then $\pm 1[m/s^2]$. Further the misalignments can be assumed small. Therefore an appropriate initial value for the parameter vector may be

$$\hat{\theta}_0 = \begin{bmatrix} 1 & 1 & 1 & 0 & 0 & 0 & 0 & 0 & 0 & \sigma^2 \end{bmatrix}^T. \qquad (15)$$

4. CRAMÉR RAO LOWER BOUND

When evaluating the performance of an estimator often it is of interest to compare the obtained estimation error with that of an optimal (unbiased with minimum variance) estimator. The optimal estimator may not exist, be unknown, or too complex to implement, still the performance of the optimal estimator only depends on the properties of the signal model [11], and may therefore be calculated independently. Given the probability distribution function of the observed data, the Cramér-Rao bound (CRLB) sets the lower limit for the variance of the estimation error for all unbiased estimators. The parametric CRLB is given by [12]

$$\mathrm{var}(\hat{\theta}) = \mathrm{diag}(\mathbf{J}^{-1}(\theta)) \qquad (16)$$

where

$$\mathbf{J}(\theta)_{ij} = E\left[\frac{\partial \log(p(\mathbf{y};\theta))}{\partial\theta_i\,\partial\theta_j}\right] \qquad (17)$$

is the Fisher information matrix. Further $p(\mathbf{y};\theta)$ is the probability density function for the observed data $\mathbf{y}$, parameterized by θ. The measured output $\mathbf{y}_k$ in Figure 4 may be described as

$$\mathbf{y}_k = \mu(\theta,\mathbf{u}_k) + \mathbf{v}_k \qquad (18)$$

where the signal part $\mu(\theta,\mathbf{u}_k)$ reads

$$\mu(\theta,\mathbf{u}_k) = \mathbf{K}\,\mathbf{T}^{-1}\mathbf{u}_k + \mathbf{b}. \qquad (19)$$

The measurement noise $\mathbf{v}_k$ is assumed to be zero mean, Gaussian distributed and uncorrelated both between the sensors and in time. Collecting the measurements $\mathbf{y}_k$ and signal parts $\mu(\theta,\mathbf{s}_k)$ into two vectors,

$$\mathbf{y} = \begin{bmatrix} \mathbf{y}_0^T & \mathbf{y}_1^T & \cdots & \mathbf{y}_{M(N-1)}^T \end{bmatrix}^T \qquad (20)$$

and

$$\mu(\theta) = \begin{bmatrix} \mu(\theta,\mathbf{u}_0)^T & \mu(\theta,\mathbf{u}_1)^T & \ldots & \mu(\theta,\mathbf{u}_{M(N-1)}) \end{bmatrix}^T \qquad (21)$$

where N is the number of samples at each orientation of the platform and M the number of orientations, the vector $\mathbf{y}$ will be Gaussian distributed as $\mathbf{y} \sim N(\mu(\theta),\mathbf{C}(\theta))$. Assuming the variance of the noise from different sensor specimens to be equal, then $\mathbf{C}(\theta) = \sigma^2\mathbf{I}_{3MN}$. Here $\mathbf{I}_{3MN}$ is the identity matrix of size $3MN$. The Fisher information matrix for the general Gaussian case is given by [12]

$$\begin{aligned}\mathbf{J}(\theta)_{ij} &= \left[\frac{\partial\mu(\theta)}{\partial\theta_i}\right]^T \mathbf{C}(\theta)^{-1}\left[\frac{\partial\mu(\theta)}{\partial\theta_j}\right] \\ &+ \frac{1}{2}\mathrm{tr}\big(\mathbf{C}(\theta)^{-1}\frac{\partial\mathbf{C}(\theta)}{\partial\theta_i}\mathbf{C}(\theta)^{-1}\frac{\partial\mathbf{C}(\theta)}{\partial\theta_j}\big). \qquad (22)\end{aligned}$$

Here $\mathrm{tr}(\cdot)$, denotes the trace operation. Noting that $\mathbf{C}(\theta) = \sigma^2\mathbf{I}_{3MN}$ in the signal model, equation (17) simplifies to

$$\begin{aligned}\mathbf{J}(\theta)_{ij} &= \frac{1}{\sigma^2}\left[\frac{\partial\mu(\theta)}{\partial\theta_i}\right]^T\left[\frac{\partial\mu(\theta)}{\partial\theta_j}\right] \\ &+ \frac{3MN}{2\sigma^4}\frac{\partial\sigma^2}{\partial\theta_i}\frac{\partial\sigma^2}{\partial\theta_j}. \qquad (23)\end{aligned}$$

Further, by utilizing that $\mathbf{u}_k$ is constant for all N samples at each orientation, the Fisher information matrix may be written as

$$\mathbf{J}(\theta)_{ij} = \frac{N}{\sigma^2}\sum_{m=1}^{M}\mathbf{A}_{ij}^m + \frac{3MN}{2\sigma^4}\frac{\partial\sigma^2}{\partial\theta_i}\frac{\partial\sigma^2}{\partial\theta_j} \qquad (24)$$

where

$$\mathbf{A}_{ij}^m = \left[\frac{\partial\mu(\theta,\overline{\mathbf{u}}^m)}{\partial\theta_i}\right]^T\left[\frac{\partial\mu(\theta,\overline{\mathbf{u}}^m)}{\partial\theta_j}\right]. \qquad (25)$$

In Appendix A, the elements in the matrix $\mathbf{A}^m$ for the proposed signal model are given. Equation (16) together with (24) and (25) give the CRLB for the parameter estimation problem, under the assumption of Gaussian measurement noise and when the precise orientation of the IMU is known, i.e. there is full knowledge about $\mathbf{u}_k$. However, in the considered calibration approach the precise orientation of the IMU is unknown but the bound still provides a good benchmark when evaluating the performance of the estimator.

Table 1: Settings used in the Monte Carlo simulation. The settings were chosen too reflect the specifications in the data sheet for the ADXL 103 accelerometer. The noise variance σ^2 where set to $0.0095\,[m/s^2]$, which corresponds to a sensor bandwidth of $30\,[Hz]$.

Axis	Scaling	Bias $[m/s^2]$	Axis	Misalignment $[^\circ]$
x	1.05	0.32	α_{yz}	2
y	0.93	0.63	α_{zy}	-5
z	1.06	-0.32	α_{zx}	3

Table 2: IMU results. The average estimate of the accelerometer cluster parameters, calculated from 20 calibration of the in-house constructed IMU. At each calibration the platform was rotated into 18 different orientation and at each orientation the sensors were sampled 100 times.

Axis	Scaling	Bias $[m/s^2]$	Axis	Misalignment $[^\circ]$
x	0.998	-0.435	α_{yz}	0.026
y	0.996	0.254	α_{zy}	-0.695
z	1.008	0.099	α_{zx}	1.808

5. RESULTS

5.1 Performance Evaluation

The proposed calibration approach has been evaluated by Monte Carlo simulations. In the simulation, the estimation of the accelerometer cluster parameters were studied when the IMU was rotated into 18 different orientations, as proposed in [4]. However, a uniformly distributed error between $[-5^\circ, 5^\circ]$ was added to the proposed orientations to reflect the relaxed demands of a precise orientation. In Figure 5(a), 5(b) and 5(c) the empirical mean square error for the scale-factors, misalignment angles and biases estimates are shown, calculated from 1000 simulated calibrations using the proposed calibration approach. The solid line is the CRLB for the calibration, when the the precise orientation of the IMU is known. In Table 1, the settings used in the simulation are summarized.

As can be seen from Figure 5(a), 5(b) and 5(c) the performance of the proposed calibration procedure is approximately 2, 8 and 5 decibel bellow the CRLB for the scale factors, misalignments and biases, respectively. Still the root mean square error, when 100 samples are taken at each orientation, of the estimated parameters are less than 10^{-2} of the magnitude of the parameters, and may therefore normally be considered acceptable for low-cost applications.

5.2 Calibration of IMU

The accelerometer cluster of the in-house constructed IMU has been calibrated using the proposed method. The IMU was by hand placed into 18 different positions, the six sides and the twelve edges of the IMU. At each orientation 100 samples were taken. In Table 2, the average parameter estimate out of 20 calibrations are shown. All the obtained estimates are in the expected region for the used sensors, that is the scale factor diverge less than 6% from the unit gain and the biases are less then $1[m/s^2]$. The estimated misalignment angle α_{yz}, as can be seen in Figure 2(b) corresponds to the misalignment between the x- and y-axis in the IMU, which should be close to zero. This is due to the fact that the x- and y-accelerometers are mounted into the same MEMS sensor case. The remaining two misalignments angles correspond to the misalignment between the x- and z-axis respectively y- and z-axis, which due to the impreciseness when the IMU was constructed, should be much larger. See Figure 1.

6. CONCLUSIONS

A MEMS sensor based inertial measurement unit has been constructed in-house, intended to be used in a low-cost GNSS aided inertial navigation systems. In order to improve the performance of the GNSS aided INS, which is highly dependent on the accuracy of the IMU, an approach for calibrating the IMU, requiring no mechanical platform for the accelerometer calibration and only a simple rotating table for the gyro calibration has been studied. The performance of the calibration algorithm is compared with the Cramér-Rao bound for the traditional case when a mechanical platform is used to calibrate the IMU, rotating the IMU into different precisely controlled orientations. Simulation results shows that the mean square error of the parameter estimates of the senor model increases with up to 8 decibel, when utilizing the proposed method. Further, not all parameters in the gyro sensor model are observable with the proposed calibration approach, increasing the computational complexity of the GNSS aided INS. Still the proposed method can be considered acceptable and useful for many low-cost applications where the cost of constructing a mechanical platform many times can exceed the cost of developing the inertial measurement unit.

A. APPENDIX

The nonzero elements for $\mathbf{A}^m$ are

$$
\begin{aligned}
\mathbf{A}^m_{1,1} &= (\bar{u}^m_x + \alpha_{zy}\bar{u}^m_y + (\alpha_{yz}\alpha_{zx} - \alpha_{zy})\bar{u}^m_z)^2 \\
\mathbf{A}^m_{1,4} &= (\bar{u}^m_x + \alpha_{zy}\bar{u}^m_y + (\alpha_{yz}\alpha_{zx} - \alpha_{zy})\bar{u}^m_z)(k_x\bar{u}^m_y + \alpha_{zx}k_x\bar{u}^m_z) \\
\mathbf{A}^m_{1,5} &= (\bar{u}^m_x + \alpha_{zy}\bar{u}^m_y + (\alpha_{yz}\alpha_{zx} - \alpha_{zy})\bar{u}^m_z)(-k_x\bar{u}^m_z) \\
\mathbf{A}^m_{1,6} &= (\bar{u}^m_x + \alpha_{zy}\bar{u}^m_y + (\alpha_{yz}\alpha_{zx} - \alpha_{zy})\bar{u}^m_z)(\alpha_{yz}k_x\bar{u}^m_z) \\
\mathbf{A}^m_{1,7} &= (\bar{u}^m_x + \alpha_{zy}\bar{u}^m_y + (\alpha_{yz}\alpha_{zx} - \alpha_{zy})\bar{u}^m_z) \\
\mathbf{A}^m_{2,2} &= (\bar{u}^m_y + \alpha_{zx}\bar{u}^m_z)^2 \\
\mathbf{A}^m_{2,6} &= (\bar{u}^m_y + \alpha_{zx}\bar{u}^m_z)k_y\bar{u}^m_z \\
\mathbf{A}^m_{2,8} &= (\bar{u}^m_y + \alpha_{zx}\bar{u}^m_z) \\
\mathbf{A}^m_{3,3} &= (\bar{u}^m_z)^2 \\
\mathbf{A}^m_{3,9} &= (\bar{u}^m_z) \\
\mathbf{A}^m_{4,4} &= (k_x\bar{u}^m_y + \alpha_{zx}k_x\bar{u}^m_z)^2 \\
\mathbf{A}^m_{4,5} &= (k_x\bar{u}^m_y + \alpha_{zx}k_x\bar{u}^m_z)(-k_x\bar{u}^m_z) \\
\mathbf{A}^m_{4,6} &= (k_x\bar{u}^m_y + \alpha_{zx}k_x\bar{u}^m_z)(\alpha_{yz}k_x\bar{u}^m_z) \\
\mathbf{A}^m_{4,7} &= (k_x\bar{u}^m_y + \alpha_{zx}k_x\bar{u}^m_z) \\
\mathbf{A}^m_{5,5} &= (-k_x\bar{u}^m_z)^2 \\
\mathbf{A}^m_{5,6} &= (-k_x\bar{u}^m_z)(\alpha_{yz}k_x\bar{u}^m_z) \\
\mathbf{A}^m_{5,7} &= (-k_x\bar{u}^m_z) \\
\mathbf{A}^m_{6,6} &= (\alpha_{yz}k_x\bar{u}^m_z)^2 + (k_y\bar{u}^m_z)^2 \\
\mathbf{A}^m_{6,7} &= (\alpha_{yz}k_x\bar{u}^m_z) \\
\mathbf{A}^m_{6,8} &= (k_y\bar{u}^m_z) \\
\mathbf{A}^m_{7,7} &= \mathbf{A}^m_{8,8} = \mathbf{A}^m_{9,9} = 1
\end{aligned}
$$

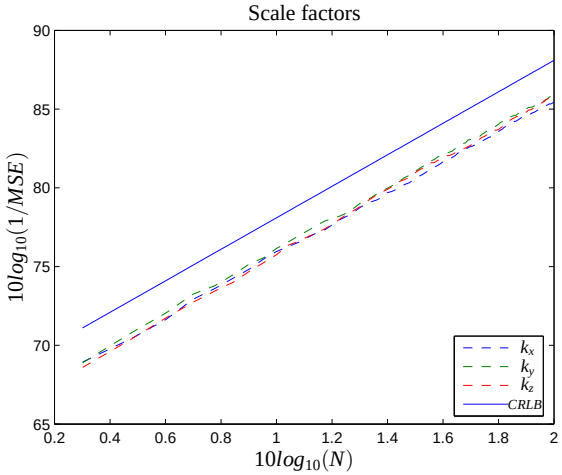

(a) Empirical MSE of the scale factor estimates as a function of the number of samples.

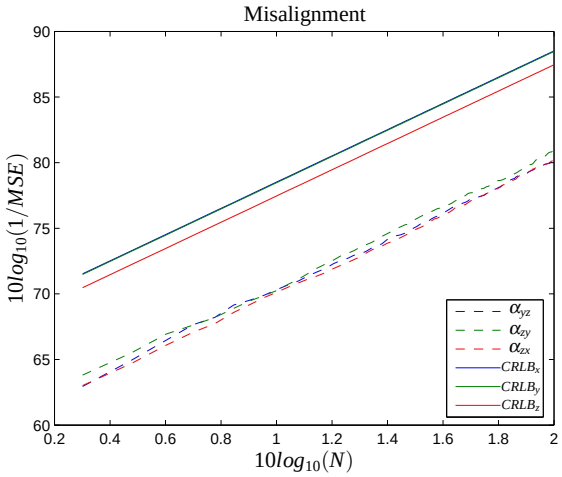

(b) Empirical MSE of the misalignment angle estimates as a function of the number of samples.

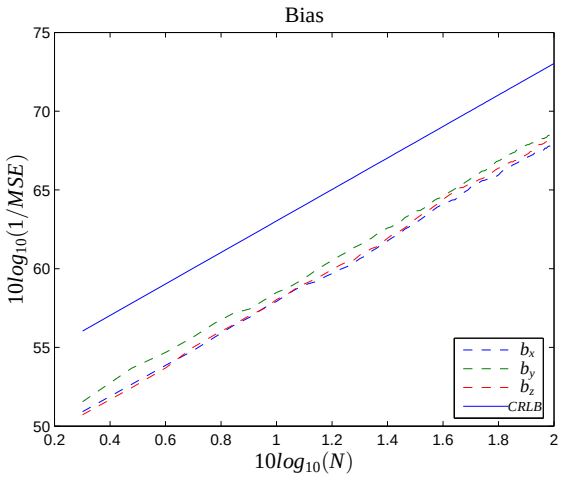

(c) Empirical MSE of the bias estimates as a function of the number of samples.

Fig. 5: Empirical mean square error for the estimation of the scale-factors, misalignments angles and biases, as a function of the number of samples at each orientation, using the proposed calibration approach. The legend CRLB indicates the Cramér Rao lower bound for the case when the precise orientation of the IMU is known.

REFERENCES

[1] **I. Skog and P. Händel "A Versatile PC-Based Platform For Inertial Navigation", in *Proc. NORSIG 2006, Nordic Signal Processing Symposium*, 7–9 June. 2006.**

[2] **N. El-Sheimy, S. Nassar and A. Noureldin "Wavelet De-Noising for IMU Alignment," in *Aerospace and Electronic Systems Magazine, IEEE*, Oct. 2004, vol. 19, Issue 10, pp. 32 – 39.**

[3] **R M. Rogers, *Applied Mathematics In integrated Navigation Systems, Second Edition*. AIAA Education Series, 2003.**

[4] **A. Chatfield, *Fundamentals of High Accuracy Inertial Navigation*. American Institute of Aeronautics and Astronautics, 1997.**

[5] **J.C. Hung, J.R. Thacher and H.V. White, "Calibration of accelerometer triad of an IMU with drifting Z -accelerometer bias", in *Proc. NAECON 1989, IEEE Aerospace and Electronics Conference*, 22–26 May. 1989, vol. 1, pp. 153 – 158.**

[6] **A. Kim and M.F Golnaraghi "Initial calibration of an inertial measurement unit using an optical position tracking system", in *Proc. PLANS 2004, IEEE Position Location and Navigation Symposium*, 26–29 April. 2004, pp. 96 – 101.**

[7] **Z.C. Wu, Z.F. Wang and Y. Ge, "Gravity based online calibration of monolithic triaxial accelermeters' gain and offset drift.", in *Proc. 4-th World Congress on Intelligent Control and Automation.*, 10–14 June. 2002.**

[8] **K.R. Britting, *Inertial Navigation Systems Analysis*. Wiley Interscience, 1971.**

[9] **M.S. Grewal, L.R. Weill and A.P Andrews *Global Positioning System, Inertial Navigation and Integration*. John Wiley and Sons, 2001.**

[10] **S. Boyd and L. Vandenberghe, *Convex Optimization*. Cambridge, 2004.**

[11] **N. Bergman, *Recursive Bayesian Estimation, Navigation and Tracking Applications*. PhD thesis, Dept. of Electrical Engineering, Linköpings Univeristy, 1999.**

[12] **S. M Kay, *Fundamentals of Statistical Signal Processing, Estimation Theory*. Prentice Hall, 1999.**